JOURNAL OF SOLID STATE CHEMISTRY 110, 290–294 (1994)

β-$BaV_2(P_2O_7)_2$: A New Polymorph of Barium Vanadium (III) Pyrophosphate Characterized by Intersecting Tunnels

Shiou-Jyh Hwu,[1] Richard I. Carroll, and Deborah L. Serra

Department of Chemistry, Rice University, P. O. Box 1892, Houston, Texas 77251

Received May 26, 1993; accepted September 15, 1993

Investigation into the synthesis of reduced vanadium phosphate has led to the formation of a new form of the barium vanadium (III) pyrophosphate compound β-$BaV_2(P_2O_7)_2$. It is a polymorph of the previously known $BaV_2(P_2O_7)_2$, which is now labeled as the α-phase. The title compound crystallizes in the $P\bar{1}$ (No. 2) space group with $a = 6.269$ (1) Å, $b = 7.864$ (3) Å, $c = 6.1592$ (9) Å, $\alpha = 101.34$ (2)°, $\beta = 105.84$ (1)°, and $\gamma = 96.51$ (2)°. The structure consists of corner-shared VO_6 octahedra and PO_4 tetrahedra that are connected in V–O–P–O–V and V–O–P–O–P–O–V bonding arrangements. This interesting three-dimensional framework is characterized by seven types of intersecting tunnels, three of which are occupied by the barium cation, while the others are empty. It is important to know that one of the empty tunnels has a relatively large window with a minimum diagonal distance of 4.41 Å, which facilitates a possible framework for a lithium ion insertion reaction. The barium atom has a 10-coordination sphere, BaO_{10}, in which the oxygen atoms can be viewed as forming two intersecting pseudohexagonal planes. β-$BaV_2(P_2O_7)_2$ appears to form at a relatively higher temperature than its polymorph, α-$BaV_2(P_2O_7)_2$. A detailed structural analysis and structural comparison with the α-phase, as well as a brief comparison with $SrV_2(P_2O_7)_2$, are presented.

INTRODUCTION

Phosphates, silicates, and silicophosphates of the early transition metals have received much attention for many years. Many of these materials are microporous solids (1) and have a variety of applications, including use as catalysts, molecular sieves, ion exchangers (2), etc. Some ion exchangers of this type have open framework structures and exhibit fast ion conduction (3, 4). The study of reduced early transition metal compounds of this kind has been extended through the use of a molten-salt flux-growth method to yield a number of interesting low-dimensional oxosilicate compounds with novel framework structures (5).

The objective of the present research is the synthesis of new forms of reduced early transition metal phosphates that possess interesting open-framework structures. It is also our intent, during the course of the study, to draw a correlation between the size and charge of the electropositive cation and framework formation. The synthesis of a new reduced titanium phosphate, $BaTi_2(P_2O_7)_2$ (6), led eventually to the study of its isostructural vanadium analogue, $BaV_2(P_2O_7)_2$ (7). The basic structure of these compounds consists of an extended $[M_2(P_2O_7)_2]^{2-}$ slab (M = Ti and V) with the barium cations residing in the tunnels formed by the MO_6 octahedra and the P_2O_7 pyrophosphate groups. The structure unit, which includes an octahedrally coordinated M, shows for the first time two "bidentate" pyrophosphate groups that are in a *cis* orientation. The reduced transition metal cation centers are isolated by the oxygens of each octahedron, which are shared only with the phosphate groups to form M–O–P–O–M and M–O–P–O–P–O–M bonds. Due to the closed-shell, nonmagnetic nature of the phosphorus cation in the $P_2O_7^{4-}$ anion, an electronic insulation (localization) with respect to the reduced transition metal centers is evident.

The structures of the pyrophosphate compounds are determined not only by the conformation variation between eclipsed and staggered pyrophosphate configurations, but also by the size and charge of the electropositive cation. Substitution of a smaller alkaline-earth cation, Sr^{2+} for Ba^{2+}, yielded a new layered compound, $SrV_2(P_2O_7)_2$ (8). This layered-type framework possesses two types of tunnel structures of which the larger tunnel is occupied by the strontium cations. The $[V_2(P_2O_7)_2]^{2-}$ structure unit is also observed, but the two "bidentate" pyrophosphate groups are in a *trans* orientation. This structure type is also adopted by $CaV_2(P_2O_7)_2$.

Repetition of the synthesis of high-yield $BaV_2(P_2O_7)_2$ produced two distinct compounds: β-$BaV_2(P_2O_7)_2$ and $Ba_3V_6(PO_4)_8$ (9). The former is a polymorph of the previously reported $BaV_2(P_2O_7)_2$, which has now been labeled as the α-phase. The formation of these two compounds, which is determined by the slightest change in reaction conditions and stoichiometry, shows a fruitful structural chemistry. In this paper, detailed synthesis,

[1] To whom correspondence should be addressed.

0022-4596/94 $6.00

structural analysis, and structural comparison of β-$BaV_2(P_2O_7)_2$ with its α-$BaV_2(P_2O_7)_2$ polymorph and the known compound $SrV_2(P_2O_7)_2$ are discussed.

EXPERIMENTAL

Synthesis. Emerald-green irregularly shaped crystals of β-$BaV_2(P_2O_7)_2$ were obtained in a multistep reaction. First a precursor was formed of barium carbonate ($BaCO_3$, 99.9% Aesar), vanadium pentoxide (V_2O_5, Aldrich 99.6%), and dibasic ammonium phosphate ($(NH_4)H_2PO_4$, Mallinckrodt 99%). These materials were mixed in a stoichiometric ratio of 5 : 3 : 20, respectively. This mixture was ground in an agate mortar and heated to 550°C in air to drive off CO_2, H_2O, and NH_3. The reduction reaction was carried out in a sealed evacuated silica tube. Vanadium metal (Aldrich 99.5%) was added to the intimate mixture of the phosphate precursor "$BaV_{1.6}(P_2O_7)_2$" so that the total reactant ratio became 5 : 3 : 20 : 4, respectively. The reaction was heated to 900°C in a temperature programmable furnace, held there for 3 days, and then slowly cooled. The green material produced was reground and reheated using the same program. XRD powder patterns indicated that the known α-$BaV_2(P_2O_7)_2$ was present in this material, along with a second phase which was later identified as $Ba_3V_6(PO_4)_8$. Following the second heating, the green product was ground with five times by weight barium chloride ($BaCl_2 \cdot 2H_2O$, EMScience 99%, dried and stored in dry box prior to use) and sealed in an evacuated silica tube which contained a coating of pyrolyzed graphite on its inner surface. The reaction took place in a box furnace at 1100°C. A malfunction in the temperature controller of the box furnace caused the furnace to heat up beyond the softening point of the silica tubes, yet the container remained intact. The reaction products were recovered by filtrating and washing off the $BaCl_2$ flux with water. The product contained a number of green crystals in what appeared to be three phases. The approximate yield of single crystal products was 40% of yellowish green α-$BaV_2(P_2O_7)_2$, 30% of β-$BaV_2(P_2O_7)_2$, and 30% of dark-green $Ba_3V_6(PO_4)_8$, along with some unidentified brown polycrystalline material.

Structure determination. Single-crystal X-ray diffraction for the structure of the title compound was carried out on a Rigaku AFC5S four-circle diffractometer. Diffraction data were collected at room temperature and crystallographic data are summarized in Table 1. The unit cell parameters and the orientation matrix for data collection were determined by a least-squares fit of 25 peak maxima with $7° < 2\theta < 24°$. There was no detectable decay during the data collection, according to the intensities of three standard reflections (0, 1, −1; −1, 0, 0; 0, −1, −1) which were measured every 150 reflections. Structure solution was carried out using the TEXSAN software package (10). Data reduction, intensity analysis, and extinction conditions were determined with the program PROCESS. Lorentz-polarization and empirical absorption corrections based on three computer chosen azimuthal scans (2θ = 14.23, 19.15, 26.93°) were applied to the intensity data. The atomic coordinates were determined using the SHELXS-86 program (11). The structures and displacement parameters were then refined by full-matrix least-square methods. The atomic coordinates and isotropic thermal parameters are listed in Table 2.

TABLE 1
Crystallographic Data for β-$BaV_2(P_2O_7)_2$

Formula mass (amu)	587.11
Space group	*P*-1 (No. 2)
Cell parameters	
a (Å)	6.269 (1)
b (Å)	7.864 (3)
c (Å)	6.1592 (9)
α (degrees)	101.34 (2)
β (degrees)	105.84 (1)
γ (degrees)	96.51 (2)
V (Å^3)	281.9 (1)
Z	1
T (K) of data collection	296
ρ calc. (g cm^{-3})	3.46
Radiation (graphite monochromated)	Mo$K\alpha$ (λ = 0.71069 Å)
Crystal shape, color	Chunk, emerald green
Crystal size (mm)	0.20 × 0.20 × 0.25
Linear abs. coeff. (cm^{-1})	56.68
Transmission factors	0.67–1.00
Scan type	$\omega - 2\theta$
Scan speed (deg. min^{-1})	4.0
Scan range (deg.)	−0.36 to 0.36 in ω
Background counts	¼ scan range on each side of reflection
2θ (max)	55°
Data collected	$h, \pm k, \pm l$
p for σ (F^2)	0.06
No. of unique data ($F_0^2 > 0$)	1290
No. of unique data with $I > 3\sigma(I)$	1243
F_{000}	274
$R(F^2)/R_w(F^2)$/GOF	0.038/0.056/1.70
$R_{int}(F^2)$	0.015
Secondary extinction coefficient	1.01 (3) × 10^{-4}
No. of variables	98

STRUCTURE DESCRIPTION AND DISCUSSION

The structure of the title compound consists of corner-shared VO_6 octahedra and P_2O_7 pyrophosphate groups, as shown in Fig. 1 by the polyhedral drawing of the unit cell, along with a barium cation residing at the origin. In the unit cell each pyrophosphate group, serving as a

TABLE 2
Positional and Equivalent Displacement Parameters for β-$BaV_2(P_2O_7)_2$

Atom	x	y	z	B_{eq} (Å^2)[a]
Ba	0	0	0	1.15 (2)
V	0.3068 (1)	0.77203 (9)	0.6215 (1)	0.55 (3)
P (1)	0.2466 (2)	0.3339 (1)	0.4803 (2)	0.58 (3)
P (2)	0.4669 (2)	0.8070 (1)	0.1829 (2)	0.60 (3)
O (1)	0.2335 (5)	0.5212 (4)	0.4708 (5)	0.95 (9)
O (2)	0.0217 (5)	0.2180 (4)	0.4324 (5)	0.91 (8)
O (3)	0.3612 (5)	0.2400 (4)	0.3146 (5)	0.87 (8)
O (4)	0.3979 (4)	0.3422 (4)	0.7407 (5)	0.78 (8)
O (5)	0.3231 (5)	0.7350 (4)	0.9340 (5)	0.94 (8)
O (6)	0.3571 (5)	0.0324 (4)	0.7815 (5)	0.90 (8)
O (7)	0.3082 (5)	0.8418 (4)	0.3301 (5)	0.84 (8)

[a] Equivalent isotropic thermal parameters defined as $B_{eq} = (8\pi^2/3)$ trace U.

"bidentate" ligand, shares two waist oxygen atoms, O(3) and O(7), of the VO_6 octahedron to form a $VO_4(P_2O_7)$ structure unit. Two structure units in the unit cell are symmetry related by an inversion center and are connected through the vertex oxygen atom, O(1), of the octahedron. There is no sharing of oxygen atoms between neighboring VO_6 octahedra. The VO_6 octahedra are, in other words, completely isolated from each other by the P_2O_7 groups, a situation which is similar to many other pyrophosphate compounds that have been reported (4, 6, 8, 12). In any case, the framework is extended through interconnecting the structure units by sharing corner oxygen atoms O(2), O(5), and O(6).

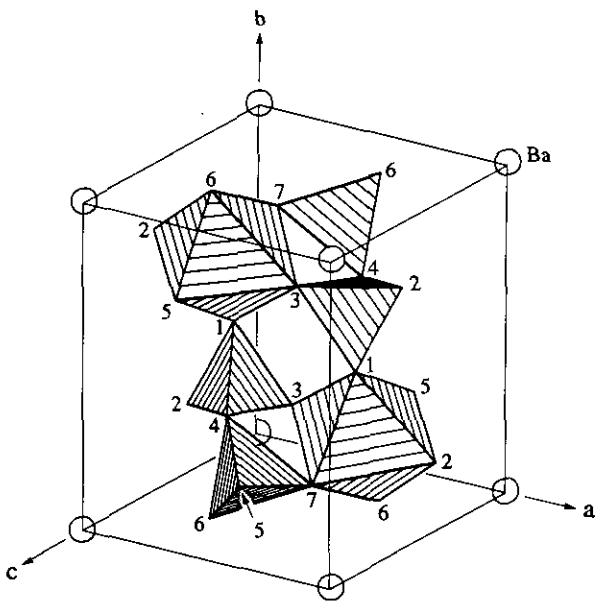

FIG. 1. The polyhedral drawing of the unit cell of β-$BaV_2(P_2O_7)_2$. The VO_6 octahedra and PO_4 tetrahedra are centered by V and P, respectively. The corners are labeled according to the numerical sequence of the oxygen atoms listed in Table 2.

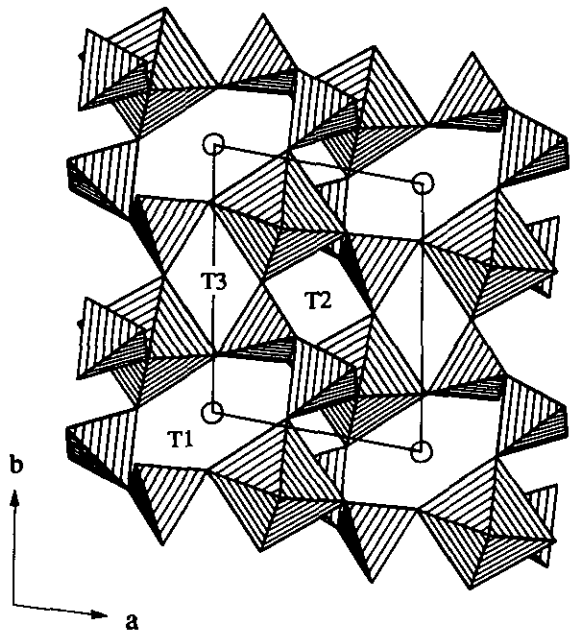

FIG. 2. Polyhedral view of the *ab* plane of β-$BaV_2(P_2O_7)_2$, showing the windows for the T1, T2, and T3 tunnels. Note that T1 contains the Ba cation, represented by open circles.

This three-dimensional structure is rarely seen in that the framework is characterized by seven types of interesting tunnels. Each type of tunnel structure is defined by its distinctly shaped window, which is formed by the edges of 4–8 polyhedra. In Fig. 2, the structure is projected onto the *ab* plane and shows the windows of three parallel tunnel structures. Two of these tunnels (T1 and T2) have pseudohexagonal windows and one (T3) has a diamond-shaped window. The tunnel with a larger pseudohexagonal window, T1, is occupied by the barium cation, while the two smaller ones, T2 and T3, are empty. These window sizes, defined by the shortest diagonal distance of the projected windows, are 3.47, 2.92, and 2.98 Å, respectively.

The above mentioned tunnels in fact intersect with other tunnel structures in the extended framework. Four types (T4–7) of additional tunnels are identified, as shown by the polyhedral drawings projected onto the *ac* (Fig. 3a) and *bc* (Fig. 3b) planes, where T4 and T5–7 are labeled, respectively. From these two polyhedral drawings, one can immediately recognize that each of the two windows for the tunnels T4 and T5 is centered by the barium cation. This indicates that the T4 and T5 tunnels are stuffed and intersect the previously mentioned T1 tunnel at the lattice origin where the barium cation resides. The T6 and T7 tunnels, on the other hand, are empty. The T6 tunnel

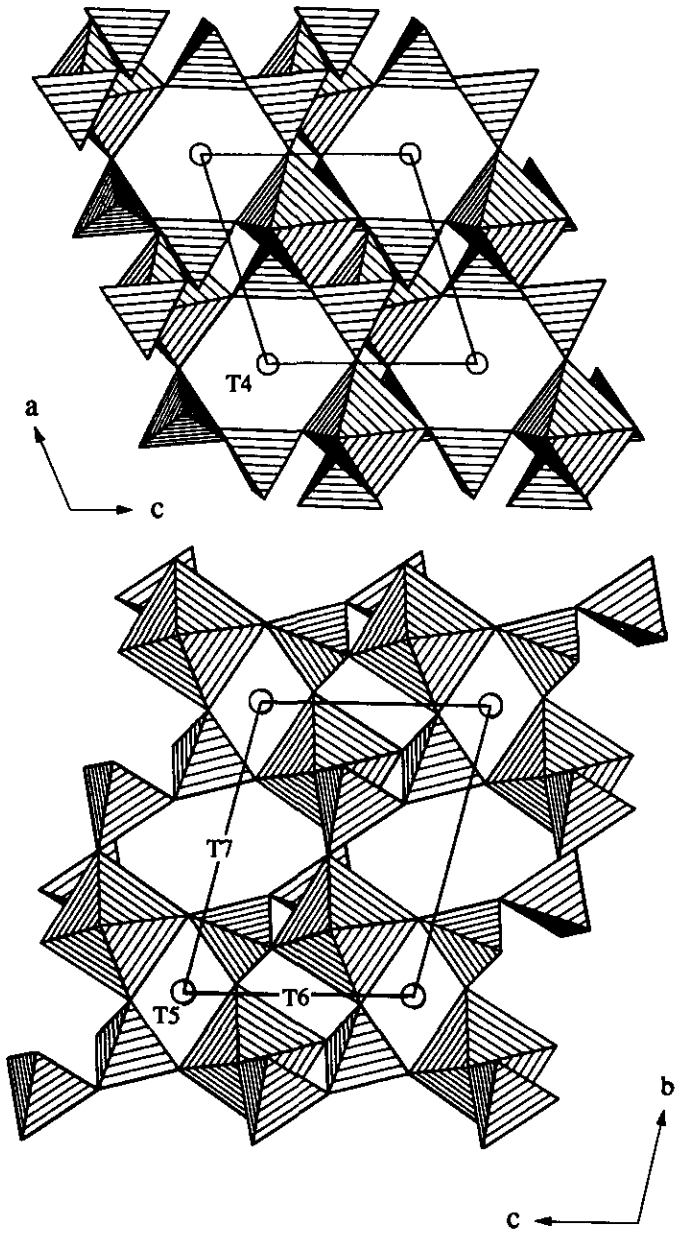

FIG. 3. Polyhedral view of the (a) *ac* and (b) *bc* planes of β-$BaV_2(P_2O_7)_2$.

intersects T1 at (0, 0, $\frac{1}{2}$), while the T7 tunnel intersects T2 at ($\frac{1}{2}$, $\frac{1}{2}$, 0) and T3 and T4 at (0, $\frac{1}{2}$, 0). It is important to note that the tunnel T7, identified in Fig. 3b, possesses a relatively large pseudo-octagonal window with the shortest diagonal distance 4.41 Å. This distance is greater than 4.32 Å (2 × Li–O distance, according to the six coordinated Shannon crystal radii (13)), which facilitates a possible framework for a lithium cation intercalation reaction.

Table 3 lists some important bond distances and angles that describe the geometry of the VO_6 octahedron and the P_2O_7 fused tetrahedra in the title compound. These values are comparable to those previously reported in both α-$BaV_2(P_2O_7)_2$ (7) and $SrV_2(P_2O_7)_2$ (8). In the VO_6 octahedron, the V–O bond distances range from 1.95 to 2.04 Å in the β-phase and 1.96–2.06 and 1.94–2.09 Å for the two known phases, respectively. Although the P–O(4)^b bridging bond distances are longer than the P–O^t terminal bond distances in the pyrophosphate polyhedron, the observed values in the title compound, 1.59–1.61 vs 1.50–1.53 Å, are very comparable to that of the reported phases, i.e., 1.59–1.61 vs 1.50–1.52 Å and 1.60–1.61 vs 1.50–1.53 Å, respectively. The bond valence analysis (14) based upon these observed bond distances produces a vanadium valence of 3.03 and phosphorus valences of 5.02 for P(1) and 4.98 for P(2), which correspond to the charge-balanced formula β-$BaV_2(P_2O_7)_2$ with trivalent vanadium and pentavalent phosphorus cations.

TABLE 3
Important Bond Distances (Å) and Angles (deg.) for β-$BaV_2(P_2O_7)_2$

	VO_6 Octahedron		
V–O (1)	1.951 (3)	V–O (5)	1.980 (3)
V–O (2)	2.007 (3)	V–O (6)	2.038 (3)
V–O (3)	2.027 (3)	V–O (7)	1.979 (3)
O (1)–V–O (2)	90.5 (1)	O (2)–V–O (7)	92.8 (1)
O (1)–V–O (3)	89.4 (1)	O (3)–V–O (5)	98.7 (1)
O (1)–V–O (5)	94.3 (1)	O (3)–V–O (6)	95.1 (1)
O (1)–V–O (6)	175.2 (1)	O (3)–V–O (7)	89.0 (1)
O (1)–V–O (7)	93.1 (1)	O (5)–V–O (6)	84.2 (1)
O (2)–V–O (3)	178.2 (1)	O (5)–V–O (7)	172.4 (1)
O (2)–V–O (5)	88.5 (1)	O (6)–V–O (7)	88.5 (1)
O (2)–V–O (6)	85.0 (1)		
	PO_4 Tetrahedra in P_2O_7 Units		
P (1)–O (1)	1.496 (3)	P (2)–O (4)	1.594 (3)
P (1)–O (2)	1.511 (3)	P (2)–O (5)	1.507 (3)
P (1)–O (3)	1.526 (3)	P (2)–O (6)	1.518 (3)
P (1)–O (4)	1.609 (3)	P (2)–O (7)	1.531 (3)
O (1)–P (1)–O (2)	114.5 (2)	O (4)–P (2)–O (5)	107.4 (2)
O (1)–P (1)–O (3)	114.2 (2)	O (4)–P (2)–O (6)	106.3 (2)
O (1)–P (1)–O (4)	105.6 (2)	O (4)–P (2)–O (7)	109.0 (2)
O (2)–P (1)–O (3)	106.2 (2)	O (5)–P (2)–O (6)	113.9 (2)
O (2)–P (1)–O (4)	108.6 (2)	O (5)–P (2)–O (7)	107.5 (2)
O (3)–P (1)–O (4)	107.4 (2)	O (6)–P (2)–O (7)	112.6 (2)
	P (1)–O (4)–P (2)	125.1 (2)	
	BaO_{10} Polyhedron		
	Ba–O (2)	2.830 (3) (2×)	
	Ba–O (3)	2.764 (3) (2×)	
	Ba–O (5)	3.112 (3) (2×)	
	Ba–O (6)	2.922 (3) (2×)	
	Ba–O (7)	2.968 (3) (2×)	
O (2)–Ba–O (3)	51.45 (9)	O (3)–Ba–O (6)	72.35 (9)
O (2)–Ba–O (5)	55.62 (8)	O (3)–Ba–O (7)	66.19 (9)
O (2)–Ba–O (6)	56.68 (8)	O (5)–Ba–O (6)	52.92 (8)
O (2)–Ba–O (7)	78.49 (9)	O (5)–Ba–O (7)	47.46 (8)
O (3)–Ba–O (5)	89.39 (9)	O (6)–Ba–O (7)	86.24 (8)

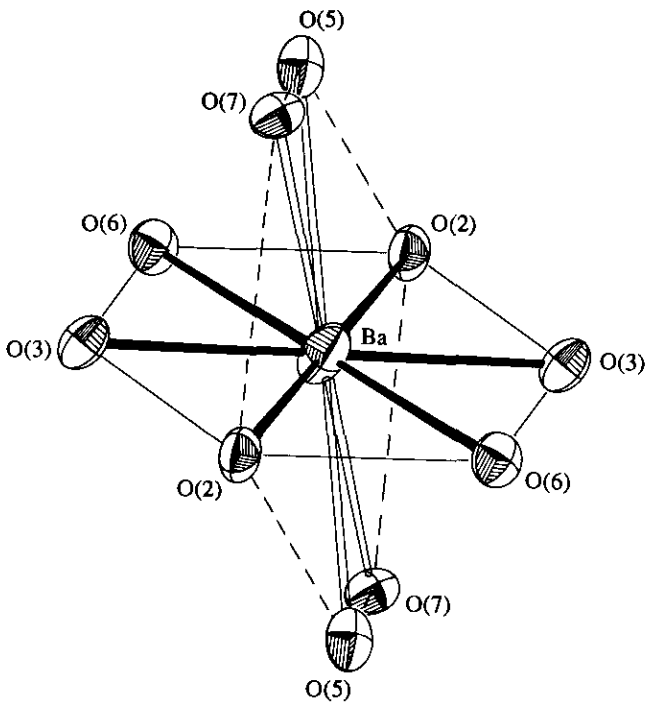

FIG. 4. ORTEP drawing (90% probability) of the BaO_{10} coordination sphere.

One of the interesting features of the β-$BaV_2(P_2O_7)_2$ structure is its coordination sphere with respect to the barium cation. This coordination sphere can be recognized as a BaO_{10} polyhedron that is defined by two intersecting planes of oxygen atoms. In Fig. 4, 10 oxygens around the barium atom are outlined by dotted and solid lines showing two approximately hexagonal planes that intersect at O(2)–Ba–O(2). Plane one is formed by 2 × (O(2), O(3), and O(6)) and plane two is formed by 2 × (O(2), O(5), and O(7)). The two planes are identified from the sum of the angles between the Ba–O bonds; i.e., the O–Ba–O bond angles add up to 360.96° for plane one and 363.14° for plane two (Table 3). The nearly 360° angles indicate that the oxygens involved are coplanar. Furthermore, plane one (outlined by solid lines) is formed by the shorter Ba–O bonds (thick bonds) while plane two (dotted lines) includes two pairs of longer Ba–O bonds (hollow bonds), with distances ranging from 2.76 to 2.92 Å and 2.83 to 3.11 Å, respectively. Nevertheless, the Ba–O bond distance range, 2.76–3.11 Å, is comparable to that observed in α-$BaV_2(P_2O_7)_2$, 2.80–3.06 Å.

The title compound is similar to α-$BaV_2(P_2O_7)_2$ and $SrV_2(P_2O_7)_2$ in one major respect: the P_2O_7 pyrophosphates form bidentate groups to "chelate" to the VO_6 octahedra. The difference lies in the fact that there is only one vanadium site per asymmetrical unit in the title compound, and it is in the singly bidentate $VO_4(P_2O_7)$ unit. In the related compounds, two vanadium sites per asymmetrical unit are found; one VO_6 octahedron shares oxygen atoms with two bidentate pyrophosphate groups while the other shares with monodentate P_2O_7 groups. This difference results in an overall structure dissimilarity between the title and related compounds in that β-$BaV_2(P_2O_7)_2$ forms an open-framework structure with both filled and empty tunnels as opposed to the α-$BaV_2(P_2O_7)_2$ and $SrV_2(P_2O_7)_2$ phases which are characterized as layered frameworks with filled tunnels. Subsequently, the calculated densities of the two polymorphous $BaV_2(P_2O_7)_2$ compounds are different, i.e., 3.71 g cm^{-3} for the stuffed α-phase vs 3.46 g cm^{-3} for the β-phase. Structurally, the frameworks of the α- and β-phases are significantly different; thus it is predicted that the activation energy for the phase transformation is high. We gather from the reaction conditions that the title compound is a high temperature phase (>1200°C). Synthesis of a high yield of the β-phase beyond 1200°C will be carried out so that low-temperature lithium intercalation reactions can be performed in order to prepare lower-valent vanadium phases.

ACKNOWLEDGMENT

Financial support by the National Science Foundation for this research (DMR-9208529) and for the single crystal X-ray diffractometer is gratefully acknowledged.

REFERENCES

1. (a) R. C. Haushalter and L. A. Mundi, *Chem. Mater.* **4,** 31 (1992); (b) G. Huan, A. J. Jacobson, J. W. Johnson, and D. P. Goshorn, *Chem. Mater.* **4,** 661 (1992); (c) G. Huan, A. J. Jacobson, and V. W. Day, *Angew. Chem. Int. Ed. Engl.* **30,** 422 (1991); (d) G. Huan, V. W. Day, A. J. Jacobson, and D. P. Goshorn, *J. Am. Chem. Soc.* **113,** 3188 (1991).
2. A. Clearfield, *Chem. Rev.* **88,** 125 (1988).
3. (a) H. Y.-P. Hong, *Mater. Res. Bull.* **11,** 173 (1976); (b) J. B. Goodenough, H. Y.-P. Hong, and J. A. Kafalas, *Mater. Res. Bull.* **11,** 203 (1976).
4. (a) S. Wang and S.-J. Hwu, *J. Solid State Chem.* **90,** 377 (1991); (b) S. Wang and S.-J. Hwu, *Chem. Mater.* **4,** 589 (1992); (c) B. Wang, M. Greenblatt, S. Wang, and S.-J. Hwu, *Chem. Mater.* **5,** 23 (1993).
5. (a) S. Wang and S.-J. Hwu, *J. Am. Chem. Soc.* **114,** 6920 (1992); (b) D. L. Serra and S.-J. Hwu, *J. Solid State Chem.* **101,** 32 (1992).
6. S. Wang and S.-J. Hwu, *J. Solid State Chem.* **90,** 31 (1991).
7. L. Benhamada, A. Grandin, M. M. Borel, A. Leclaire, and B. Raveau, *Acta Crystallogr. Sect. C* **47,** 2437 (1991).
8. S.-J. Hwu and E. D. Willis, *J. Solid State Chem.* **93,** 69 (1991).
9. R. I. Carroll and S.-J. Hwu, manuscript in preparation.
10. "TEXSAN: Single Crystal Structure Analysis software, version 5.0." Molecular Structure Corp., The Woodlands, TX (1989).
11. G. M. Sheldrick, in "Crystallographic Computing 3" (G. M. Sheldrick, C. Krüger, and R. Goddard, Eds.), pp. 175–189. Oxford University Press, London/New York, 1985.
12. S. Wang and S.-J. Hwu, *J. Solid State Chem.* **92,** 219 (1991).
13. R. D. Shannon, *Acta Crystallogr. Sect. A* **32,** 751 (1976).
14. I. D. Brown and D. Altermatt, *Acta. Crystallogr. Sect. B* **41,** 244 (1985).